Morphology and Mechanical Properties of Nanocomposites of Cellulose Acetate and Organic Montmorillonite Prepared with Different Plasticizers

Juliana Aristéia de Lima, Caio Augusto Pinotti, Maria Isabel Felisberti, Maria do Carmo Gonçalves

Chemistry Institute, Universidade Estadual de Campinas, PO Box: 6154, 13083-970, Campinas—SP, Brazil

Received 14 March 2011; accepted 13 June 2011
DOI 10.1002/app.35517
Published online 6 December 2011 in Wiley Online Library (wileyonlinelibrary.com).

ABSTRACT: Nanocomposites of cellulose acetate and an organically modified montmorillonite (CA/MMTO) were prepared by melt intercalation in a twin-screw extruder, using two different plasticizers: di-octyl phthalate (DOP) and triethyl citrate (TEC). The influence of plasticizer type and the organoclay added to the structure, the morphology, and the thermal properties of the nanocomposites was investigated. XRD and SAXS results indicated a significant CA or/and plasticizer intercalation in the clay gallery for the CA/MMTO nanocomposites. In addition, the images obtained by TEM show that the morphology of CA/MMTO nanocomposites is made up of intercalated and exfoliated silicate layers. The glass transition temperature (T_g) of CA with DOP or TEC decreased in at almost same value, which shows the characteristics of both additives as plasticizers for cellulose acetate chains. Tensile tests indicate that the nanocomposites with either of the two plasticizers presented the same performance with respect to material properties. The results demonstrated that, for some applications, TEC is an useful alternative to plasticize CA in order to substitute DOP, a non eco-friendly plasticizer. © 2011 Wiley Periodicals, Inc. J Appl Polym Sci 124: 4628–4635, 2012

Key words: cellulose acetate; glass transition temperature; plasticizer; nanocomposites

INTRODUCTION

Nanocomposites offer the possibility of diversification for polymer applications due to their excellent properties such as high heat distortion temperature, dimensional stability, improved barrier properties, flame retardancy, and enhanced thermomechanical properties.[1–5]

Biodegradable polymers from renewable resources are a fairly new area of nanocomposites that has attracted the attention of researchers with expertise in diverse areas.[6–13] Nanoreiforcement of bio-based polymers can be used to create new materials. Organic–inorganic materials are extraordinarily versatile as they could be formed from a large variety of biopolymers such as polysaccharides, polypeptides, proteins and nucleic acids, among others. Various nanoreinforcements are currently being developed, but the most intensively researched type of nanocomposite uses layered silicate clay mineral as the reinforcing phase due to its easy availability and low cost. Therefore, the development of biodegradable polymer-based nanocomposites can open the way toward innovative applications of polymers.[5–7,11]

Cellulosic plastics such as cellulose acetate (CA), a thermoplastic produced by the esterification of cellulose materials such as cotton, recycled paper, wood cellulose, and sugarcane have already been used in several areas, such as filters, membranes, packing films, adhesives, coatings for paper and plastic products, electrical isolation, and drug delivery systems.[14,15] CA shows poor dimensional stability and fair mechanical properties, which could be enhanced by the use of organoclay and plasticizers. Thus, CA can also be considered a good candidate for the preparation of biopolymer–clay nanocomposites owing to its potential biodegradability, excellent optical clarity, and stiffness.[16–18] Moreover, extensive efforts have been made to improve the processibility of CA by the use of appropriate plasticizers in order to increase the polymer chain flexibility and thereby facilitate more uniform mixing between the matrix and the reinforcement.[19] The effects of plasticizers on polymers have been widely investigated with several pharmaceutical applications, including those made from cellulose ethers,[20,21] poly(vinyl alcohol),[22] cellulose acetate,[23] and acrylic polymers.[24–26] These studies have mainly focused on the influence of

Correspondence to: M. do Carmo Gonçalves (maria@iqm.unicamp.br).

Contract grant sponsors: CNPq and FAPESP (Brazil) through Inomat, National Institute (INCT) for Complex Functional Materials and Petrobras-CENPES/IQ.

plasticizers on the physical and mechanical properties of the plasticized polymer used in the film coating of solid dosage forms.

Commercial cellulose acetate is processed with di-octyl phthalate (DOP) as the plasticizer. Phthalate esters have recently been investigated for environmental and health related problems due to the leaching of plasticizer from the CA matrix. On the other hand, citrate esters, like triethyl citrate (TEC), are derivatives of natural compounds and are considered eco-friendly plasticizers in the formulation of cellulosic plastics.[16] Thus, the reason for the choice of this plasticizer in this work is to compare it with commercial plasticizer (non eco-friendly). Moreover, some authors[16,27,28] evaluated the effect of TEC plasticizer in the properties of CA/clay nanocomposites and reported in their work TEC as an efficient plasticizer.

The aim of this work was the development of nanocomposites based on cellulose acetate and an organoclay using as plasticizers dioctyl phthalate and triethyl citrate in a twin-screw extruder. The structures and macroscopic properties for CA/MMTO nanocomposites were investigated. Thermal and mechanical properties were studied as a function of clay content and plasticizer type and are discussed in terms of clay dispersion.

EXPERIMENTAL

Materials

In this study, different cellulose acetates (CA) from Eastman Chemicals Co., Kingsport, Tennessee, were used: (1) CA-1 with 38.7 wt % acetyl content, number–average molar mass $\overline{M}_n = 50{,}000$ g mol^{-1}, without additives, and in powder form; (2) CA-2 with 39.8 wt % acetyl content, $\overline{M}_n = 30{,}000$ g mol^{-1}, in pellet form and containing 20 wt % of di-octyl phthalate (DOP) as plasticizer. The number–average molar mass, acetyl content, and di-octyl phthalate amount were provided by the producer. For CA-1, triethyl citrate (TEC) from Acros Organics, Morris Plains, NJ, was used as plasticizer. An organically modified montmorillonite (organo clay-MMTO) with a cation exchange capacity of 90 mequiv/100 g and a real density of 1.98 g/cm^3, commercially known as Cloisite® 30B clay was purchased from Southern Clay Products, Gonzales, Texas, USA. The ammonium cation of Cloisite® 30B is reported to be methyl tallow bis-2-hydroxyethyl quaternary ammonium.

Melt compounding and injection molding

Cellulose acetate and organoclay (MMTO) were dried under vacuum at 80°C for at least 24 h before use. TEC plasticizer (20 wt %) was added to CA-1 and mixed in a Marconi MA039 mechanical stirrer at 6000 rpm for 30 min. CA-1 or CA-2 were mixed with the desired quantity of organoclay (3 and 5 wt %) and processed in a twin-screw extruder ($L/D = 20$), *Coperion—ZSK-26 Mc*. The temperature profile was 160/170/190/230°C and with a screw rate of 250 rpm. The mass ratios of CA/organoclay were as follows: 97/3 and 95/5 wt %. Subsequently, the injection molding was performed in an *Arburg All Rounder M-250* at 230°C to obtain specimens for mechanical tests (tensile and impact geometries) with dimensions according to ASTM D-638 and ASTM D-256, respectively.

Characterization

The following characterizations were conducted in the extruded samples.

Dynamic mechanical thermal analysis (DMTA)

The specimens (8.0 × 5.0 × 1.5 mm) were subjected to a sinusoidal deformation in tension mode analysis at a frequency of 1.0 Hz, strain amplitude of 0.01%, and heating rate of 2°C min^{-1} from −100°C to 240°C in a Rheometric Scientific DMTA V Analyzer.

X-ray diffraction (XRD)

X-ray diffraction measurements were performed using a Shimadzu XRD-7000 difractometer in the reflection mode with incident Cu Kα radiation ($\lambda = 0.1540$ nm) using a 0.5°/min scan rate.

Transmission electron microscopy (TEM)

The morphology of nanocomposites was examined in a *Carl Zeiss CEM 902 transmission electron microscope*, operated at an acceleration voltage of 80 kV. Ultrathin sections, ~ 40 nm thick, were cut perpendicular to the sample plane at −140°C in a *Leica EM FC6 cryo-ultramicrotome*.

Two dimensional-small angle/wide angle X-ray scattering (2D-SAXS/WAXS)

SAXS experiments were performed using the D11A-SAXS1 beamline, with a two-dimensional imaging plate detector (2D-SAXS), at the Brazilian Synchrotron Light Source (LNLS), using a position sensitive detector for the small angle region. The wavelength used was 0.1542 nm and the sample to detector distance used was 627 nm. The measurements were collected with a two-dimensional imaging plate and the scattering profiles were obtained from radial integration of the images. The

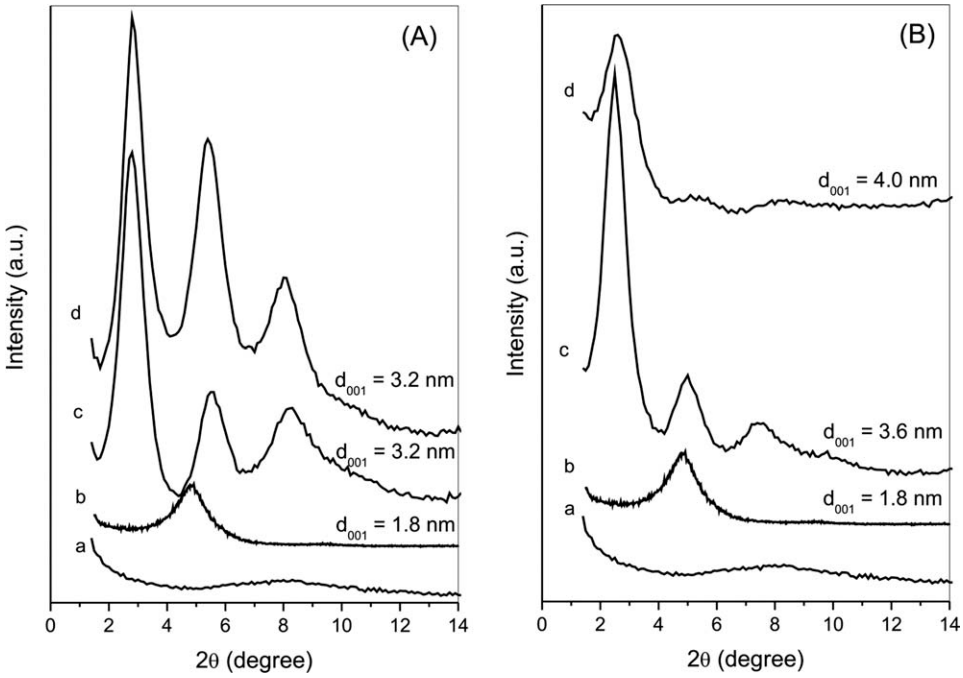

Figure 1 XRD diffraction patterns of (a) CA, (b) MMTO without plasticizer, (c) plasticized 97/3 nanocomposite, and (d) plasticized 95/5 nanocomposite. (A) Nanocomposites and CA plasticized with TEC; (B) nanocomposites and CA plasticized with DOP.

measurements were taken at 25°C and the scattering profiles were corrected for sample absorption and detector response.

RESULTS AND DISCUSSION

Microstructure of the nanocomposites

Figure 1 shows the XRD patterns of organoclay (MMTO), plasticized CA and CA/MMTO nanocomposites, with a fixed amount (20 wt %) of TEC [Fig. 1(A)] or DOP [Fig. 1(B)].

The XRD peak shifted from 4.9° (d_{001} = 1.8 nm) (Fig. 1) for pure MMTO to 2.8° (d_{001} = 3.2 nm) for 95/5 nanocomposite with TEC as a plasticizer, which suggests intercalation of CA and/or TEC in the clay galleries. As reported by Park et al.[16] in a TEC/organoclay (20/80 wt %) mixture, TEC plasticizer is able to swell the organoclay. This swelling was interpreted as plasticizer intercalation in the clay gallery as a result of the hydrogen bonding between the hydroxyl groups of TEC and the organoclay. Bonzanini et al.[27] reported that the XRD peak of the plane (001) of MMTO shifted from 4.9° (d_{001} = 1.8 nm) to 2.3° (d_{001} = 3.8 nm) for a TEC/organoclay (20/80 wt %) mixture. However, in this work, cellulose acetate was previously plasticized with TEC, followed by extrusion with clay. Thus, TEC was sorbed in the CA powder before the nanocomposite processing. Generally, the driving force for polymer intercalation in the clay galleries is a result of the enthalpic contribution related to the establishment of favorable polar polymer–surface interactions.[29] Thus, the intercalation of MMTO clay by the plasticized CA could be attributed to the interactions between the polar groups in CA (acetyl and hydroxyl groups) and the hydroxyl groups of the organoclay.[28]

Comparing both plasticizers, CA/MMTO nanocomposites prepared with DOP showed higher *d*-spacing values, which means that the diffusion of the CA chains in the clay gallery could be facilitated by this plasticizer. These results lead to the conclusion that the polymer matrix plasticization plays an important role in the clay intercalation and/or exfoliation.

All the studied compositions of CA/MMTO nanocomposites also showed a second and a third peaks, in the range of 4.0°–6.1° and 6.5°–8.7°, respectively, which are associated with collapsed MMTO formed by extraction of surfactant during the processing course.[30]

To characterize the microstructure of the clay layers in CA nanocomposites, the SAXS technique was used. Figure 2 summarizes the Lorentz's corrected intensity, $I(q) \times q$, of CA, MMTO, and CA/MMTO.

The peaks obtained from the curves indicate that the scattering vector (q) at maximum $I(q)$ is slightly shifted to lower values of q for all nanocomposites when compared with pure MMTO, independent of the plasticizer used. In the wide-angle region

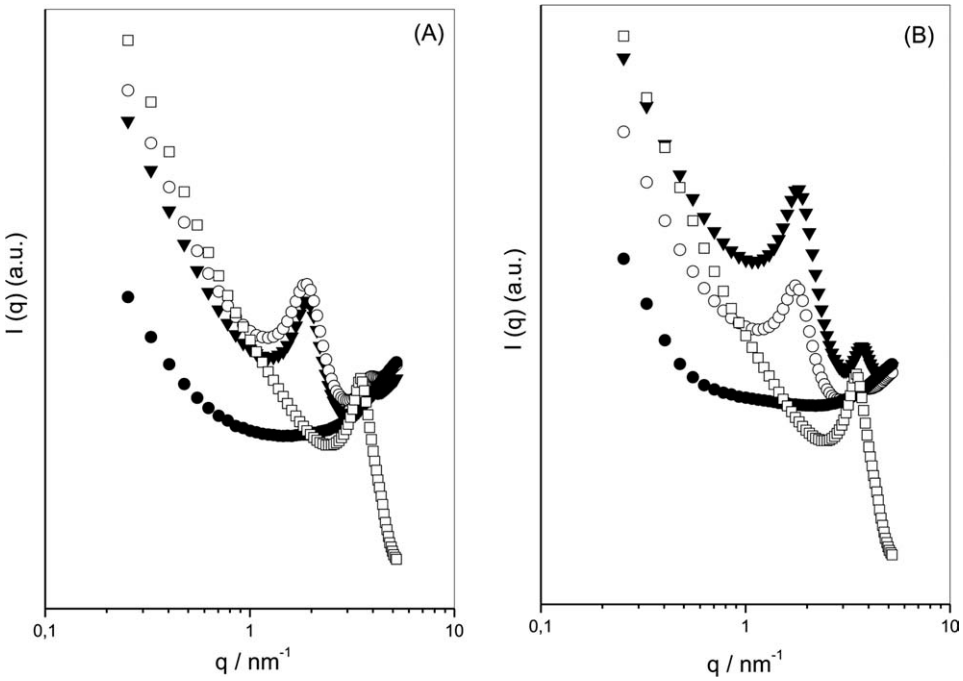

Figure 2 SAXS profiles of (●) CA, (□) MMTO without plasticizer, (○) plasticized 97/3 nanocomposite, and (▼) plasticized 95/5 nanocomposite. (A) Nanocomposite and CA plasticized with TEC; (B) nanocomposite and CA plasticized with DOP.

($q > 1$ nm^{-1}), the corresponding *d*-spacings of the different nanocomposite compositions are presented in Table I and show good agreement with the XRD results. The original *d*-spacing is 1.8 nm ($q = 3.5$ nm^{-1}) for the MMTO. Moreover, SAXS patterns provide information about the clay distribution in the polymer matrix. Due to fluctuations of electron density, the scattered X-rays give rise to characteristics patterns. The analyses of the low angle region ($q < 1$ nm^{-1}) for the CA/MMTO nanocomposites showed an angular dependence of $\alpha \sim -3$. Yoonesi et al.[31] correlated this angular dependence with platelets and tactoids of various thicknesses, which are bent and curved (fractal contribution to shape).

The 2D-SAXS patterns of CA/MMTO nanocomposites provided additional information about the clay structures in these materials. For any periodic structure, the localized sharpness of the scattering patterns reflects the extent of orientation of the stacked layers in the material.[32,33] As shown in Figure 3, CA/MMTO nanocomposites with both plasticizers

TABLE I
Organoclay Interlayer Spacing Obtained by SAXS

	Di-octyl phthalate (DOP)		Triethyl citrate (TEC)	
CA/MMTO	q_{max} (nm^{-1})	d-spacing (nm)	q_{max} (nm^{-1})	d-spacing (nm)
97/3	1.7	3.6	1.9	3.3
95/5	1.8	3.4	1.9	3.3

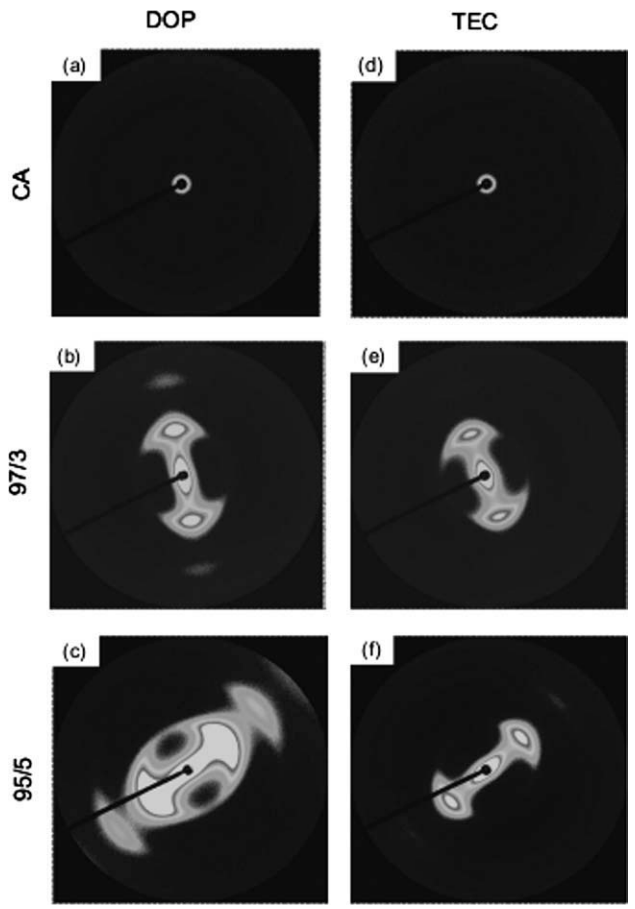

Figure 3 2D-SAXS patterns for CA with DOP or TEC and 97/3 and 95/5 CA/MMTO nanocomposites with DOP or TEC.

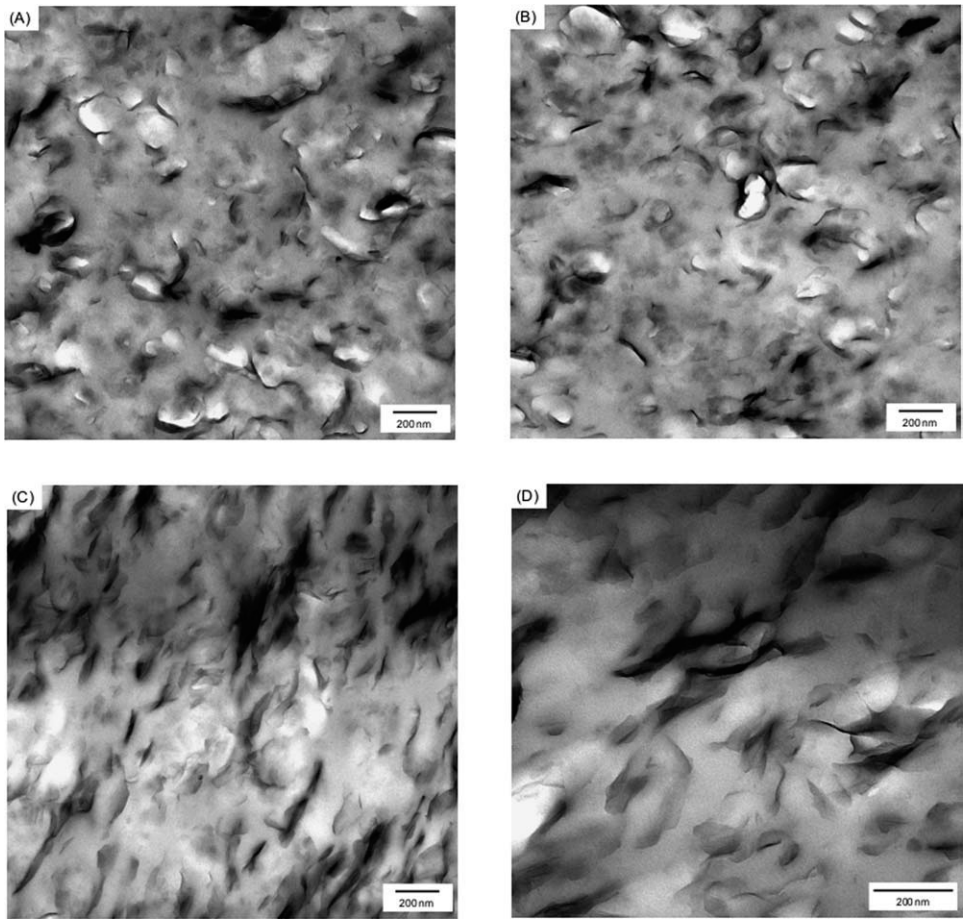

Figure 4 TEM micrographs of the 95/5 CA/MMTO nanocomposites with both plasticizers: (A) and (B) DOP (different regions of the same sample); (C) and (D) TEC (different regions of the same sample).

presented an anisotropic pattern suggesting that the clay layers are aligned in a preferential direction.

The central rings illustrated within the patterns, Figure 3(b, c, e and f), are deformed and correspond more appropriately to an ellipse. This shape can be associated with the distortion of the clay lamellae arrangement in the CA matrix. Thus, the effect of shearing imposed during sample processing promotes lamellae orientation and causes the crystallographic domain deformations along the main macroscopic axis. The SAXS results suggest that the morphologies of the CA/MMTO consist of aligned silicate layers.

While XRD and SAXS can provide highly accurate information on the platelet separation distance, the TEM can directly reveal spatial distribution of the dispersed, intercalated, and exfoliated structures.[34] TEM micrographs of nanocomposites with 5 wt % MMTO content are presented in Figure 4.

The images in Figure 4 show a good clay dispersion (no large aggregates), independent of the plasticizer. Furthermore, there are exfoliated structures. CA/MMTO nanocomposites with DOP as the plasticizer, Figure 4 (A,B), show higher clay exfoliation and distribution than the nanocomposites with TEC, Figure 4 (C,D).

TEM images also show good adhesion at the clay–polymer interfaces. Moreover, CA/MMTO nanocomposites showed some tactoids, which interact to form geometrically curved structures.

Dynamic mechanical properties

In DMA analyses, the glass transition temperature (T_g) was assumed to be the temperature corresponding to the maximum of the peaks in the loss modulus (E'') as a function of temperature. Figure 5(B) shows the loss modulus curves ($E'' \times T$) for CA and CA/MMTO nanocomposites. The curves are shifted from each other. The glass transition temperatures obtained from $E'' \times T$ are presented in Table II.

The glass transition temperature (T_g) of the pure CA without plasticizer was 170°C (data obtained by differential scanning calorimetry—DSC). From a qualitative viewpoint, the values grouped in Table II give evidence of the expected plasticizing character of DOP and TEC additives since the plasticizer incorporation reduced the T_g values. This effect can

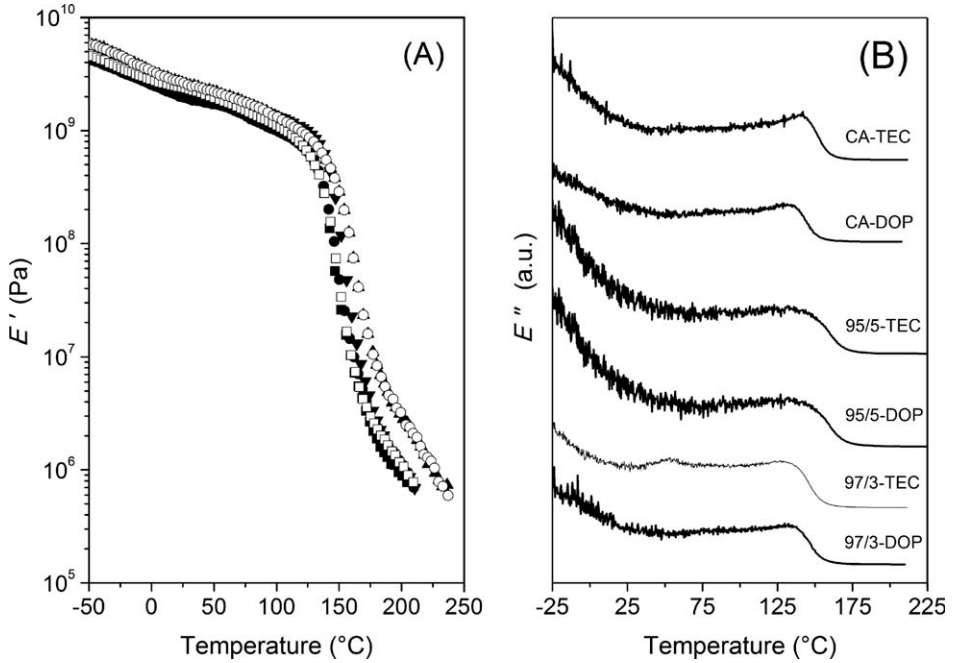

Figure 5 (A) Storage modulus (E') as a function of temperature for CA and CA/MMTO nanocomposites. (■) CA-DOP, (●) 97/3 and (▲) 95/5 AC-DOP/MMTO nanocomposites, (▼) CA-TEC, (□) 97/3 and (○) 95/5 AC-TEC/MMTO nanocomposites. (B) loss modulus (E'') as a function of temperature for CA and CA/MMTO nanocomposites.

be attributed to the additional free volume between the CA chains provided by the plasticizer, which facilitates segmental movements.[28,35,36] The result suggests that plasticizer molecules are randomly distributed within the amorphous matrix.[37] The literature describes the T_g decrease as a measure of plasticizer efficiency.[28,36,38] In this way, DOP appears to be a more effective plasticizer than TEC when both are compared on the basis of the same plasticizer amount in the compound. It is noteworthy that apart from the above, the two composition sets, one using DOP and other using TEC, used different molecular weights. Due to this, the expectation was that there might be an effect of the higher molecular weight of CA with TEC which could, in turn, cause the glass transition temperature to be higher. However, the net result showed merely a compensation effect.

Gutierrez-Rocca and McGinity[25] concluded that the efficiency of a plasticizer was related to its chemical structure and the interaction nature between polymer and plasticizer. These interactions can be estimated based on the solubility parameter considering the contribution of three components: dispersive (δ_d), permanent dipole–dipole or polar (δ_p), and hydrogen bonding (δ_h) interactions.[39] Table III lists values of these terms for CA, DOP, and TEC.

The higher values of δ_p and δ_h for DOP, compared with the corresponding values for TEC, suggest more efficient interactions between the acetyl groups in the repeat unit of CA and the carbonyl groups present in DOP. Although the plasticizer concentration in the CA matrix is the same for both DOP and TEC and equal to 20 wt %, the molar ratio of DOP to TEC is 0.70. The molar volume (V_m) of the DOP is higher than the molar volume of the TEC plasticizer, 396.5 $cm^3\ mol^{-1}$ and 243.5 $cm^3\ mol^{-1}$, respectively, and therefore, DOP should contribute more effectively to the increase of the free volume of the plasticized CA. These data allow concluding that the performance of DOP and TEC as plasticizers for CA results from the nature and magnitude of CA-

TABLE II
Glass Transition Temperatures (T_g) and Storage Modulus (E') Obtained by DMTA for CA and CA/MMTO Nanocomposites with Different Plasticizers (DOP or TEC)

Composition (CA or CA/MMTO)	DOP			TEC		
		Storage modulus (E')			Storage modulus (E')	
	T_g (°C)	50°C (GPa)	180°C (MPa)	T_g (°C)	50°C (GPa)	180°C (MPa)
CA	132	1.8	1.9	140	1.9	2.7
97/3	134	1.9	2.4	135	2.0	2.3
95/5	142	2.2	8.5	144	2.2	8.5

TABLE III
Hansen Solubility Parameters for Cellulose Acetate and the Plasticizer Used in the CA/MMTO Nanocomposites System at 25°C[39–42]

	Solubility parameters $(MPa)^{1/2}$			
Sample	δ	δ_d	δ_p	δ_h
CA	25.1	18.6	12.7	11.0
DOP	18.3	16.6	7.0	3.1
TEC	17.0	16.4	5.0	1.3

plasticizer interactions and the contribution of each plasticizer to the free volume of the polymer. Plasticized CA with higher free volume should present a lower T_g.

In relation to the CA/MMTO nanocomposites, it is not possible to obtain the solubility parameter of the organoclay but it can be considered to be a highly polar material,[40,43] which permits the development of interactions with CA and the plasticizer that have high solubility parameters, mainly through hydrogen bonding and ion–dipole interactions.

Except for the 97/3 nanocomposite with TEC as the plasticizer, the addition of organoclay changes the T_g to higher values when compared with the plasticized CA (Table II). The shift of T_g is strongly dependent on interface morphology, interparticle spacing, and polymer–nanoparticle interactions.[44] On the other hand, complex relaxation dynamics in the polymer/layered clay nanocomposites relative to the nanoparticles can be expected due to the geometrical constraint imposed by the two-dimensional space of the intercalated and exfoliated structures. The change in T_g is not only attributed to the extent of interaction between the polymer chains and layered clay but also to the confinement effect of the chains. Thus, the interplay of the confinement and surface effects imperatively dictate to T_g shift.[45,46] Moreover, the physical or chemical attachment of the polymer chains with the layered clay alters the segmental mobility due to the difference in the entanglement density and conformational entropy near the clay surface. Evidently, a strong interaction between the polymer and clay increases T_g.[47,48] Thus, in the case of CA/MMTO nanocomposites, it is possible to associate the increase of glass transition temperature to the restriction of the segmental motion of CA backbone by the organoclay (MMTO),[28,36] which indicates favorable interactions between the plasticized CA and the silicate layers. This hypothesis is reinforced by the observation of peak width of the loss modulus, corresponding to the glass transition. The peak becomes broader with the addition of clay, indicating broader relaxation spectra for nanocomposites as a consequence of the existence of polymer chains in different ambients (in bulk and at the interface particle–polymer) and chain segments attached to different particles.

Figure 5(A) shows the storage modulus (E') as a function of temperature for plasticized CA and CA/MMTO nanocomposites. A single drop in storage modulus in the range of 120°C to 160°C was observed, which is related to the glass transition of CA. The modulus values at 50°C (glassy region) and 180°C (elastic region) are given in Table II. The storage modulus of glassy CA with the addition of 3 wt % of MMTO increases $\sim$ 5%, regardless of the plasticizer used. Furthermore, 5 wt % addition of MMTO increases $E' \sim 18\%$ and 15% with the use of DOP and TEC, respectively, which could be due to reinforcement effects through the formation of efficient interactions between plasticized CA chains and MMTO at the interface. The consequences of this is also reflected in the shifting of the loss modulus (E''), Figure 5(B), peaks indicating an increase in the glass transition temperatures (T_g).

Mechanical properties

Table IV shows the Young's modulus, tensile strength, and impact resistance for CA and CA/MMTO nanocomposites in the presence of DOP or TEC.

In relation to the tensile strength and Young's modulus the mechanical properties are almost the same despite the plasticizer type and the addition of MMTO. The 95/5 nanocomposite showed a discrete decrease in Young's modulus in relation to 97/3. This behavior can be due to the less uniform distribution of clay particles in CA matrix, as observed by TEM. These results could be attributed to both plasticizers, DOP and TEC, which lead to a decrease of both tensile strength and Young's modulus. Because the plasticizer behaves like a solvent when mixed

TABLE IV
Mechanical Properties of the Injected CA and CA/MMTO Nanocomposites with Different Plasticizers

	Di-octyl phthalate (DOP)			Triethyl citrate (TEC)		
CA and CA/MMTO (wt %)	Young's modulus (MPa)	Tensile strength (MPa)	Impact resistance (KJ m^{-2})	Young's modulus (MPa)	Tensile strength (MPa)	Impact resistance (KJ m^{-2})
CA	1270 ± 65	55 ± 1	125 ± 11	1057 ± 64	54 ± 1	61 ± 6
97/3	1270 ± 62	51 ± 1	130 ± 11	1288 ± 34	55 ± 1	67 ± 5
95/5	1248 ± 60	58 ± 4	134 ± 10	1151 ± 57	59 ± 2	70 ± 2

with a polymer, the macromolecular chain cohesion is decreased and tensile strength properties are thus reduced.[49]

The addition of organoclay did not affect the impact resistance. In relation to the plasticizers, when the DOP was used, the impact resistance increased almost 100% in relation to the nanocomposites with TEC. This is due to the interactions involved in the CA–DOP interface and the good dispersion of MMTO into the matrix (CA), shown by TEM analyses.

CONCLUSIONS

XRD and SAXS analyses showed the intercalation of the CA and plasticizer mixture in the clay gallery. In addition, TEM images showed that the morphology is also made up of exfoliated silicate layers. The results showed that the confined CA/plasticizer chains interact with the clay surface through polar and hydrogen bonds, which are responsible for clay–CA interfacial adhesion.

The impact resistance for the CA and CA/MMTO nanocomposites is higher when DOP was used as the plasticizer. On the other hand, tensile tests indicated that the properties of the materials prepared with DOP and TEC are very similar, which demonstrates that for some applications TEC is a useful alternative for CA plasticization in order to substitute a non eco-friendly plasticizer with a more eco-friendly one.

References

1. LeBaron, P. C.; Wang, Z.; Pinnavaia, T. J. Appl Clay Sci 1999, 15, 11.
2. Ray, S. S.; Yamada, K.; Okamato, M.; Ueda, K. Polymer 2003, 44, 857.
3. Fornes, T. D.; Yoon, P. J.; Hunter, D. L.; Keskkula, H.; Paul, D. R. Polymer 2002, 43, 5915.
4. Fornes, T. D.; Paul, D. R. Polymer 2003, 44, 3945.
5. Alexandre, M.; Dubois, P. Mater Sci Eng 2000, 28, 1.
6. Ruiz-Hitzky, E.; Darder, M.; Aranda, P. J Mater Chem 2005, 15, 3650.
7. Wang, X. Y.; Du, Y. M.; Luo, J. W. Carbohydr Polym 2007, 69, 41.
8. Zhuang, H.; Zheng, J. P.; Gao, H. J Mater Sci Mater Med 2007, 18, 951.
9. Shih, Y. F.; Wang, T. Y.; Jeng, R. J. J Polym Environ 2007, 15, 151.
10. Ray, S. S.; Okamoto, M. Prog Polym Sci 2003, 28, 1539.
11. Ray, S. S.; Bousmina, M. Prog Mater Sci 2005, 50, 962.
12. Fomin, V. A.; Guzeev, V. V. Prog Rubber Plast Technol 2001, 17, 186.
13. Wibowo, A. C.; Misra, M.; Park, H. M.; Drzal, L. T.; Schlek, R.; Mohanty, A. K. Compos A: Appl Sci Manufact 2006, 37, 1428.
14. Balser, K.; Eicher, T.; Wnadel, M.; Astheinmer, H. J. In: Gerhartz, W.; Yamamoto, Y. S., Eds.; Cellulose Esters. Ullmann's Encyclopedia of Industrial Chemistry, vol. A5. VCH; Weinheim, Germany, 1986; 438–457.
15. Edgar, K. J.; Buchanan, C. M.; Debenham, J. S.; Rundquist, P. A.; Seiler, B. D.; Shelton, M. C. Prog Polym Sci 2001, 26, 1605.
16. Park, H. M.; Misra, M.; Drzal, L. T.; Mohanty, A. K. Biomacromolecules 2004, 5, 2281.
17. Wang, X. Y.; Du, Y. M.; Luo, J. W. Carbohydr Polym 2007, 69, 41.
18. Kim, J.; Yun, S. Macromolecules 2006, 39, 4202.
19. Ayuk, J. E.; Mathew, A. P.; Oksman, K. J Appl Polym Sci 2009, 114, 2723.
20. Bodmeier, R.; Paeratakul, O. Int J Pharm 1994a, 103, 47.
21. Rowe, R. C.; Kotaras, A. D.; White, E. F. T. Int J Pharm 1984, 22, 57.
22. Lim, L. Y.; Wan, S. C. Drug Dev Ind Pharm 1994, 2, 1007.
23. Guo, J. Drug Dev Ind Pharm 1993, 19, 1541.
24. Bodmeier, R.; Paeratakul, O. Int J Pharm 1993, 96, 129.
25. Gutierrez-Rocca, J. C.; McGinity, J. W. Int J Pharm 1994, 103, 293.
26. Lin, S.; Lee, C.; Lin, Y. Pharm Res 1991, 8, 1137.
27. Romero, R. B.; Alves, R. N. V.; Gonçalves, M. C. Barrier Properties and Morphology of Cellulose Acetate Nanocomposites; 11th International Conference on Advanced Materials, Rio de Janeiro, Brazil, 2009; A544.
28. Park, H. M.; Liang, X.; Mohanty, A. K.; Misra, M.; Drzal, L. T. Macromolecules 2004, 37, 9076.
29. Vaia, R.; Giannelis, E. Macromolecules 1997, 30, 7990.
30. Gatos, K. G.; Karger-Kocsis, J. Polymer 2005, 46, 3069.
31. Yoonessi, M.; Toghiani, H.; Daulton, L. T.; Lin, J.-S.; Pittman, C. U. Macromolecules 2005, 38, 818.
32. Bafna, A.; Beaucage, F.; Mirabela, F.; Mehta, S. Polymer 2003, 44, 1103.
33. Kaneko, M. L. Q. A.; Romero, R. B.; Gonçalves, M. C.; Yoshida, I. V. P. Eur Polym J 2010, 46, 881
34. Yalcin, B.; Cakmak, M. Polymer 2004, 45, 6623.
35. White, L. A. J Appl Polym Sci 2004, 92, 2125.
36. Park, H. M.; Mohanty, A. K.; Drzal, L. T.; Lee, E.; Mielewski, D. F.; Misra, M. J Polym Environ 2006, 14, 27.
37. Dubault, A.; Bokobza, L.; Gandin, E.; Halary, J. L. Polym Int 2003, 52, 1108.
38. Rahman, M.; Brazel, C. S. Prog Polym Sci 2004, 29, 1223.
39. Hansen, C. M. Hansen Solubility Parameters; CRC Press: Boca Raton, 2000.
40. Bonzanini, R. R.; Leite, C. A. P.; Gonçalves, M. C. Polymer 2009, 50, 161.
41. Adamska, K.; Voelkel, A.; Héberger, K. J Chromatogr A 2007, 1171, 90.
42. Wypych, G. Handbook of Plasticizers; ChemTec Publishing: New York, 2004.
43. Jang, B. N.; Wang, D.; Wilkie, C. A. Macromolecules 2005, 38, 6533.
44. Khan, A. N.; Hong, P.-D.; Chuang, W.-T.; Shih, K.-S. Polymer 2009, 50, 6287.
45. Narayanan, R. A.; Thiyagarajan, P.; Lewis, S.; Bansal, A.; Schadler, L. S.; Lurio, L. B. Phys Rev Lett 2006, 97, 075505.
46. Tsui, O. K. C.; Russell, T. P.; Hawker, C. J. Macromolecules 2001, 34, 5535.
47. de Gennes, P. G. Eur Phys J 2000, 2, 201.
48. Brown, H. R.; Russell, T. P. Macromolecules 1996, 29, 798.
49. Százdi, L.; Pozsgay, A.; Pukánszky, B. Eur Polym J 2007, 43, 345.